PROCEEDINGS OF SPIE

SPIEDigitalLibrary.org/conference-proceedings-of-spie

Q-parametric estimations for the turbulent characteristics of a thermodynamically inhomogeneous non-stationary optical path

Blank, A., Suhareva, N., Tsyganov, M.

A. V. Blank, N. A. Suhareva, M. V. Tsyganov, "Q-parametric estimations for the turbulent characteristics of a thermodynamically inhomogeneous non-stationary optical path," Proc. SPIE 11560, 26th International Symposium on Atmospheric and Ocean Optics, Atmospheric Physics, 1156011 (12 November 2020); doi: 10.1117/12.2574989

Event: 26th International Symposium on Atmospheric and Ocean Optics, Atmospheric Physics, 2020, Moscow, Russian Federation

Q-parametric estimations for the turbulent characteristics of a thermodynamically inhomogeneous non-stationary optical path

A. V. Blank, N. A. Suhareva, and M. V. Tsyganov

Moscow State M.V. Lomonosov University, Physics Faculty, Russia, 119991, Moscow, Leninskie Gory 1-2

ABSTRACT

An analysis technique is described within of the non-extensive Tsallis thermodynamics for experimentally recorded time scans, for displacement vectors, and for the drift velocity of the beam energy center. The variations of the Boltzmann-Gibbs entropy, the q-deformed Tsallis entropy and the available states number of the statistical ensemble of the recorded positions of the collimated wave beam energy center and its drift velocity are determined. To determine the type of attractors of the studied stochastic process, the spectra of Lyapunov exponents for the positional parameters of the wave beam are analyzed.

Keywords: Non-extensive thermodynamics, q-entropy Tsallisa, escort distribution, energy distribution, Lyapunov parameters

1. INTRODUCTION

The traditional approach adopted in the Bolman-Gibbs thermodynamics is not applicable in the long paths analysis, since the basic assumption that all cells of the phase volume are equally accessible is incorrect because of spatial thermal inhomogeneity, non-equilibrium, and unsteadiness of the propagation environment of the signal beam. In fact, in classical thermodynamics there are no forbidden states and the probability of visiting available sites is leveled. The natural consequence of such models is the canonical distribution for the population probability of a particular state as a function of the energy value.[1,2]

Non-equilibrium, inhomogeneous, and non-stationary systems have a different type of phase space that allows interaction with delay, non-local interactions, and multifractal structure.[3,4] The consequence of the phase space modification will be a loss of additivity for a number of thermodynamic characteristics, primarily for internal energy, temperature and entropy.[5,6] The observed characteristics of physical systems are modified, but in the limit of transition to continuous, smooth, and Euclidean phase space, they coincide with traditional.[7–9]

Define the main accents in the observed experimental characteristics:

- multimodality of the distribution functions of the positional characteristics of the collimated beam at the output of the path,
- examples of the variation kinetics of the q-deformed Tsallis entropy during daylight hours, informativeness of experimentally determined q-entropy as a measure of system disequilibrium and non-extension,
- escort distribution profiles allowing to determine the ensemble average of allowed states value of measured states,
- q-deformed energy distribution profiles for various potentials,
- micro-time variations of the maximum Lyapunov exponent determining the time of stochastic quasistationary system,
- the spectrum evolution of Lyapunov exponents, indicating the preservation of the global stochastic structure (hyperhaos).

Further author information: (Send correspondence to A. V. Blank)
A. V. Blank : E-mail: BlankArkadiy@physics.msu.ru

26th International Symposium on Atmospheric and Ocean Optics, Atmospheric Physics, edited by Gennadii G. Matvienko, Oleg A. Romanovskii, Proc. of SPIE Vol. 11560, 1156011

· doi: 10.1117/12.2574989

2. ENSEMBLE OF STATES COLLIMATED WAVE BEAM

The experimental series obtained on the long path described in detail earlier in the work.[10,11] Define the experimental control modes:

- the beam profile used is single-mode Gaussian,
- "path length" collimated beam - 1350 m,
- registration aperture through diffused frosted glass - 256x256 mm^2,
- resolution of the technical vision camera - 1 pt/mm,
- frame exposure – from 10 μs to 100 μs depending on conditions,
- polling frequency – from 125 Hz to 3 kHz,
- video series duration – up to 10000 frames.

Each video sample is considered as a statistical ensemble of the intensity distributions realizations and kinematic characteristics of the wave beam energy center. We define a set of controlled characteristics for each frame and a pair of neighboring frames:

- radius vector and its components for the energy center position of the beam,
- if the task allows you to set the target coordinate, the displacement of the energy center from the target coordinate is controlled,
- vector drift velocity of the energy center,
- drift velocity components.

To analyze the statistical properties of recorded video samples, are defined a spatial discretization grid, each of whose cells corresponds to the available states for the energy center of the wave beam in the registration plane. The grid pitch vertically and horizontally is defined in 2 mm, the binding to the vertical and horizontal directions is justified by the preferential direction of convective currents initiated by the temperature gradient (vertical) and the direction of the wind load (horizontal). Given the known distribution of the wave beam intensity in the registration plane, the components of the displacement vector of the energy center $xC,\ yC$ are determined as follows:

$$xC = \frac{\sum_{i=1}^{256} c * I(c,r)}{\sum_{i=1}^{256} I(c,r)}, \quad yC = \frac{\sum_{i=1}^{256} r * I(c,r)}{\sum_{i=1}^{256} I(c,r)}, \tag{1}$$

here (c, r) are the numbers of columns and rows in the array of the video selection frame.

Almost all of the analyzed samples in both directions are characterized by multimodal distributions, regardless of the time of day and the type of the analyzed characteristic — displacement or drift velocity.

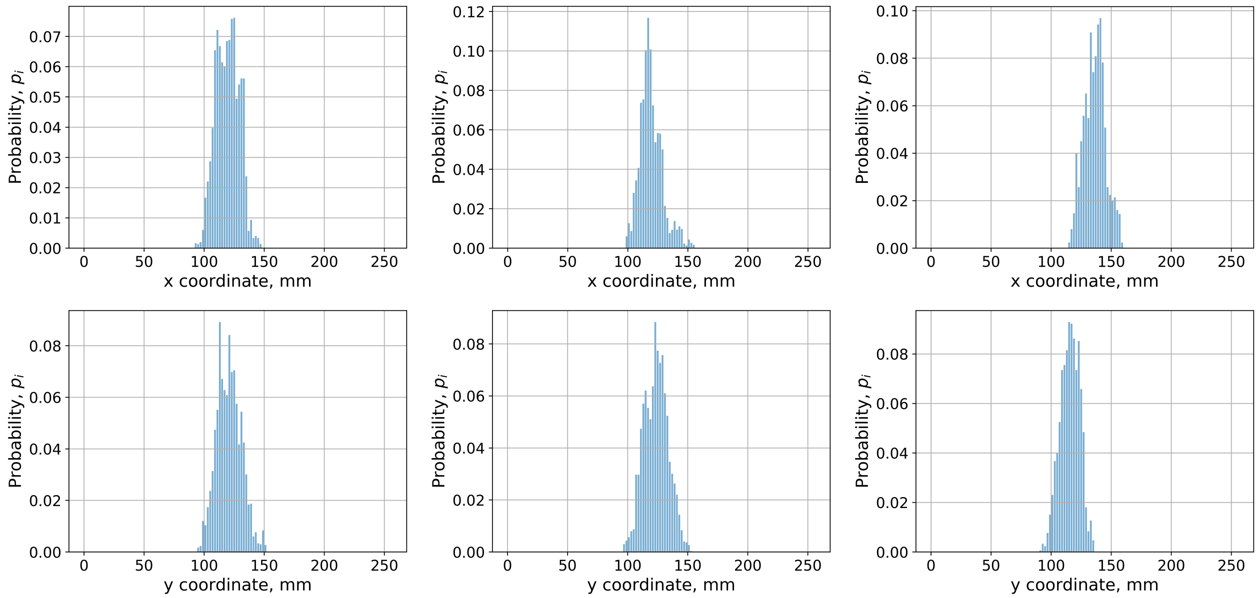

Figure 1. Probability distribution functions for horizontal (top row) and vertical offsets (bottom row)

3. ENTROPY OF TSALLIS

We define the q - parametric Tsallis entropy as follows:[3, 12]

$$S_q = -k_B \frac{1 - \sum_{i=1}^{W} p_i^q}{1-q}, \tag{2}$$

for $q \to 1$ the expression goes over into the formula for the Boltzmann-Gibbs entropy.

An estimate of the "deformation" q parameter can be performed, to a first approximation, based on the value of the average and dispersion of the distribution function over inverse temperatures:

$$q = \frac{<\beta^2>}{<\beta>^2} = \frac{\sigma^2}{\beta_0^2} + 1. \tag{3}$$

The assessment is obviously valid for small values of internal energy compared with the "thermal gap", in the system under study:

$$E << k(T_{max} - T_{min}), \Rightarrow B(E) = e^{-\beta_0 E}\left[1 + \frac{1}{2}(q-1)\beta_0^2 E^2 + \dots\right]. \tag{4}$$

Consider the variations of the Tsallis entropy and the Boltzmann-Gibbs entropy reconstructed from a series of experimental samples for two consecutive days at the end of April 2019. The first of two days was clear, the second cloudy. The processing used four time series corresponding to the components of the displacement vector and the velocity vector of the energy center of the collimated wave beam.

In Fig.2 and Fig.3 q-strain values from 0 to 1.5 were used with step of 0.5. We give the main properties of the obtained distributions:

- $q = 0$ – the value of the Tsallis entropy is one less than the number of available states,
- $q = 0.5$ – q-deformation increases the contribution of unlikely states and reduces the contribution of highly probable states, the sum of the corresponding components becomes more than one,

- $q = 1$ – the Tsallis entropy value coincides with the Boltzmann-Gibbs entropy value,
- $q = 1.5$ – q-deformation reduces the contribution of unlikely states and increases the contribution of highly probable states, the sum of the corresponding components becomes more than one.

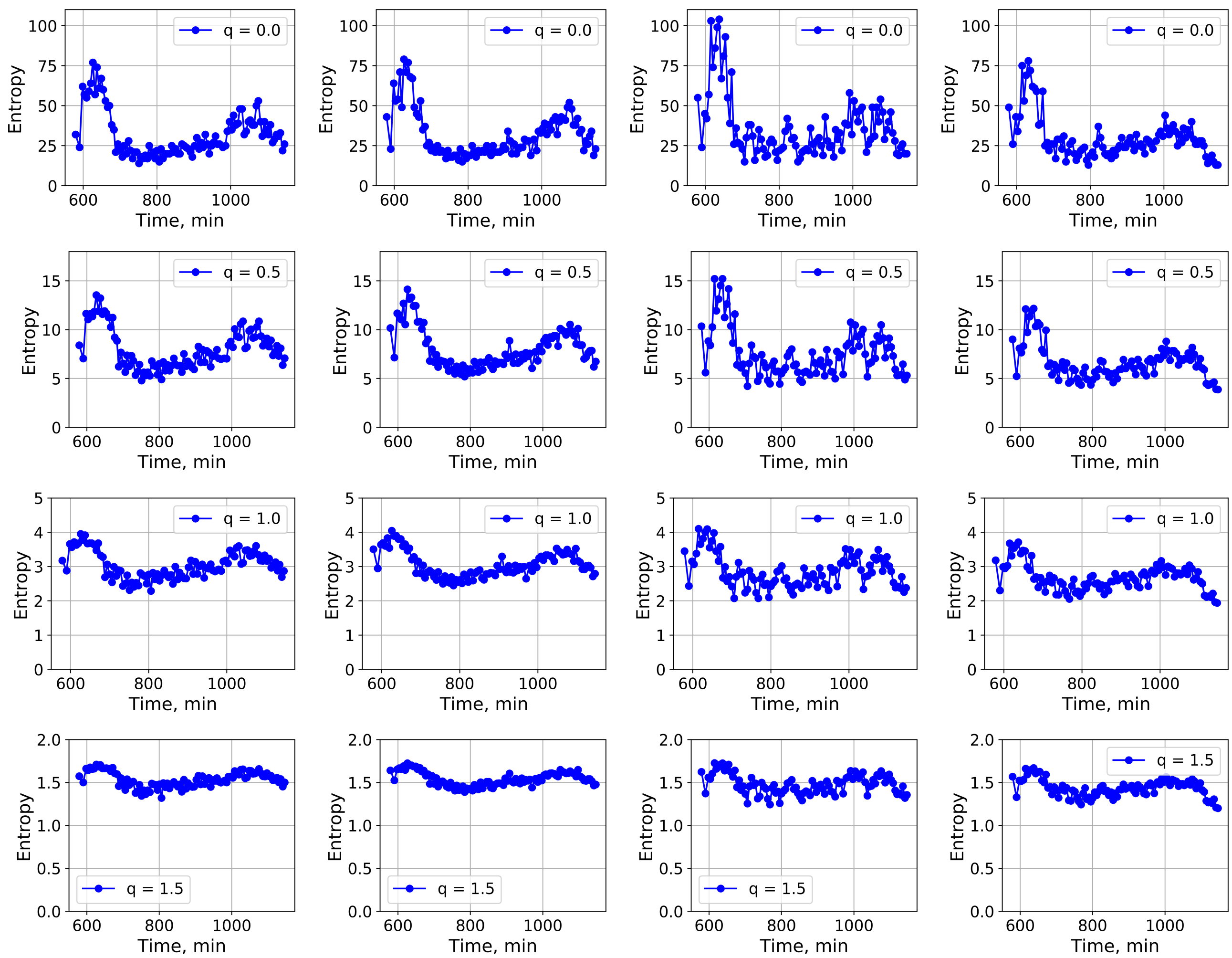

Figure 2. Variation of q-entropy at q = 0, 0.5, 1.0, and 1.5 for April 29, 2019

Strong variations in the q-parametric entropy of the system under study can be related to its non-additivity for independent systems. For example, for a two-component system whose states are described by a joint multiplicative distribution:[13, 14]

$$p(\vec{r}_1; \vec{r}_2) = p_1(\vec{r}_1) p_2(\vec{r}_2), \tag{5}$$

where $p_1(\vec{r}_1)$, $p_2(\vec{r}_2)$ belong to independent q-systems, the entropy of the total system is defined as follows:

$$S_q(p(\vec{r}_1; \vec{r}_2)) = S_q(p_1(\vec{r}_1)) + S_q(p_2(\vec{r}_2)) + \frac{1-q}{k_B} S_q(p_1(\vec{r}_1)) S_q(p_2(\vec{r}_2)) \tag{6}$$

If the subsystems under consideration are dependent, the relation is valid with the use of conditional probability distributions:

$$S_q(p(\vec{r}_1; \vec{r}_2)) = S_q(p_1(\vec{r}_1)) + S_q(p_2(\vec{r}_2)|p_1(\vec{r}_1)) = S_q(p_2(\vec{r}_2)) + S_q(p_1(\vec{r}_1)|p_2(\vec{r}_2)). \tag{7}$$

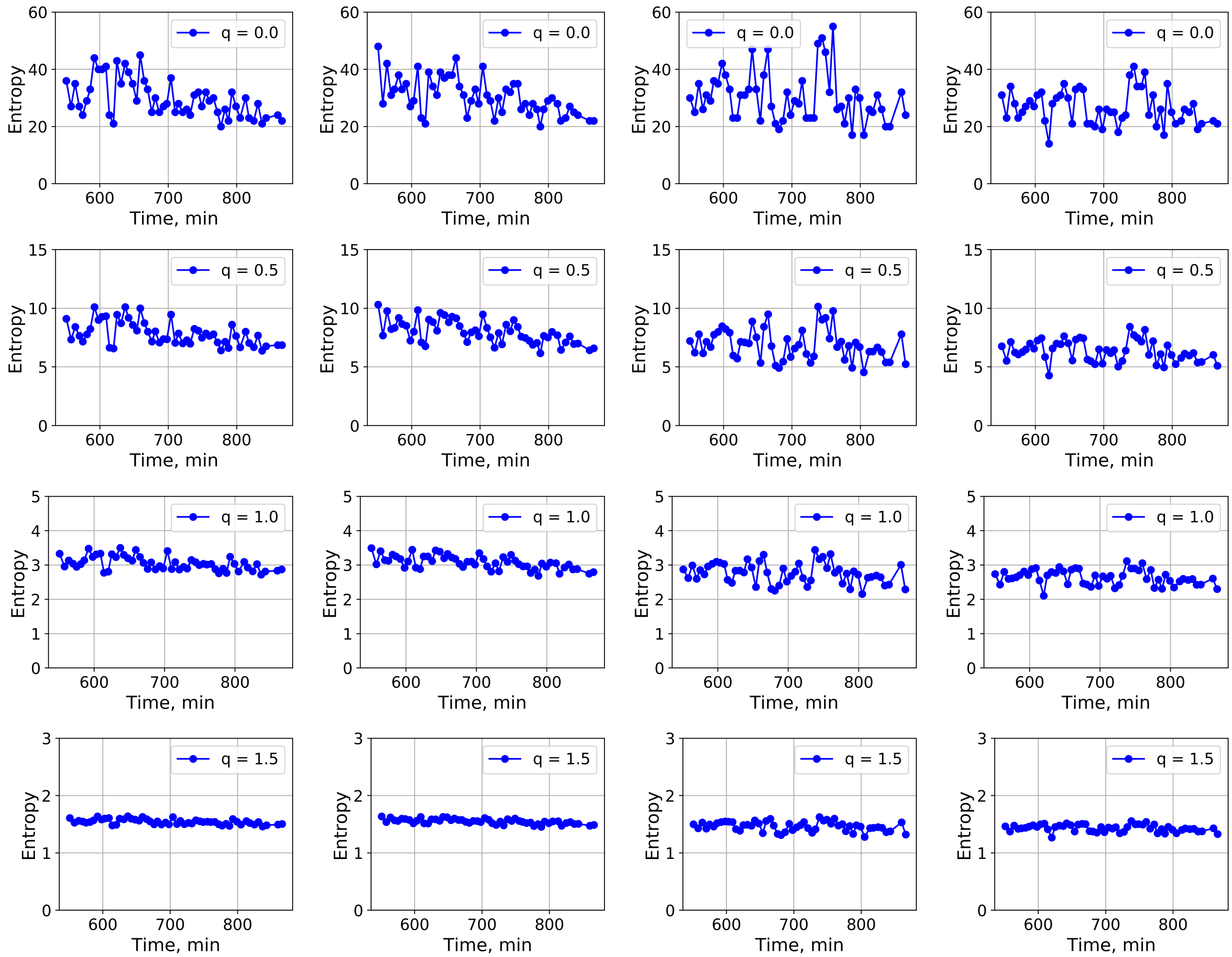

Figure 3. Variation of q-entropy at q = 0, 0.5, 1.0, and 1.5 for April 30, 2019

Modes are possible in which conditional probability $p_1(\vec{r}_1)|p_2(\vec{r}_2) = p_2(\vec{r}_2)$ or $p_2(\vec{r}_2)|p_1(\vec{r}_1) = p_1(\vec{r}_1)$. For such modes, the term "pseudo-additivity" is introduced.[2]

4. Q-PARAMETRIC ESCORT DISTRIBUTIONS

The q-deformation of the probability distribution function to violates the original normalization. To compensate for such violations, an apparatus of escort characteristics calculated for each q value is proposed. Define escort distribution for the q-deformed probability so:[2,15]

$$P_i(q) = \frac{p_i^q}{\sum_{i=1}^{W} p_i^q} = \frac{p_i^q}{Z_q} \tag{8}$$

here Z_q is the generalized q-parametric statistical sum.

q-deformed normalized distribution can be written as:

$$\sum_{i=1}^{W} P_i(q) = 1, \tag{9}$$

Based on the escort probability distribution, we determine the q-deformed value of the system internal energy:

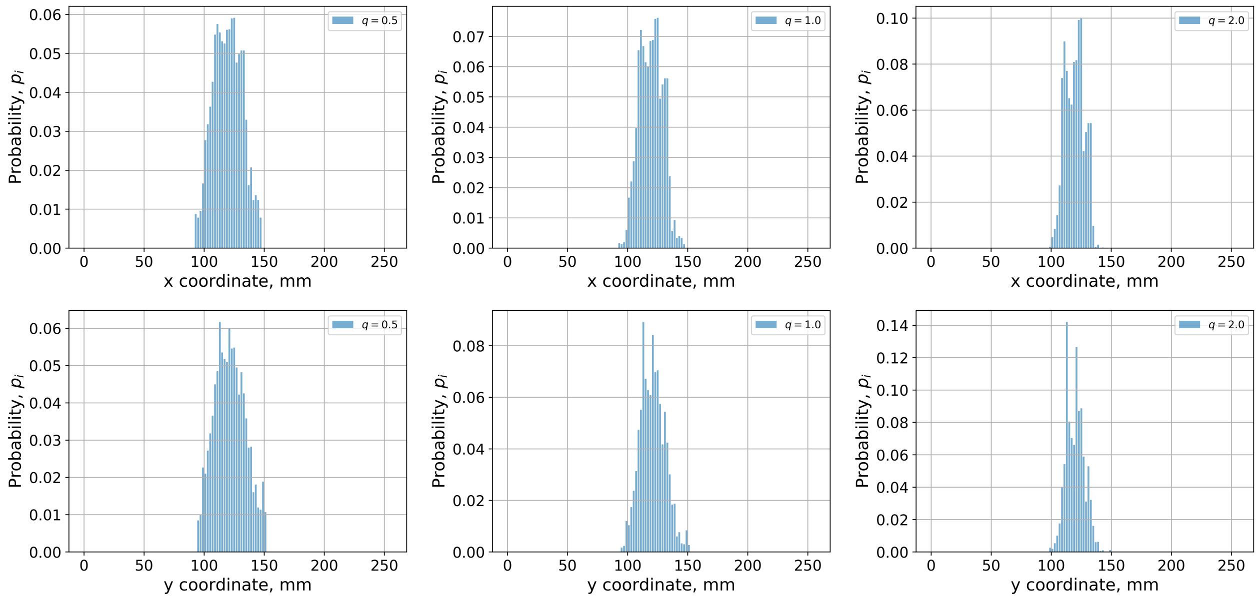

Figure 4. Escort distribution profiles for q = 0.5 (left) and q = 2.0 (right). The initial distribution is in the center.

$$\sum_{i=1}^{W} P_i(q) E_i = U_q, \tag{10}$$

where E_i are the system energy levels.

Examples of q-deformed escort distributions for q = 0.5, 1.0, and 2.0 are shown in Fig.4.

5. Q-PARAMETRIC FAMILIES OF ENERGY DISTRIBUTIONS

The modification of the escort probability distributions profile with a change in the q-parameter is accompanied by a change in the internal energy of the system while saving values the energy levels:[1,15,16]

$$U_q = \frac{\sum p_i^q E_i}{\sum p_i^q}. \tag{11}$$

We write the q-deformed energy distribution:

$$\tilde{p}_i = \frac{1}{\tilde{Z}_q} \left[1 - (1-q)\tilde{\beta}_q (E_i - U_q)\right]^{\frac{q}{1-q}}. \tag{12}$$

here Z_q is the q-deformed statistical sum –

$$\tilde{Z}_q = \sum_{i=1}^{W} [1 - (1-q)\tilde{\beta}_q (E_i - U_q)]^{\frac{q}{1-q}}, \tag{13}$$

β_q – q - deformed average value of the inverse temperature:

$$\beta_q = \frac{\beta_0}{\sum_{i=1}^{W} p_i^q}. \tag{14}$$

Let the "deformation energy" of a collimated wave beam can be expanded in a series in degrees of displacement from the unperturbed position of the beam axis.

$$E_i = \kappa_1 \rho + \kappa_2 \rho^2 + ..., \quad \rho = \left| xC_i - \overline{xC} \right|. \tag{15}$$

Let's define the q-deformed internal energy according to (11) and construct a family of characteristics for the linear and quadratic approximations for the Hamiltonian.

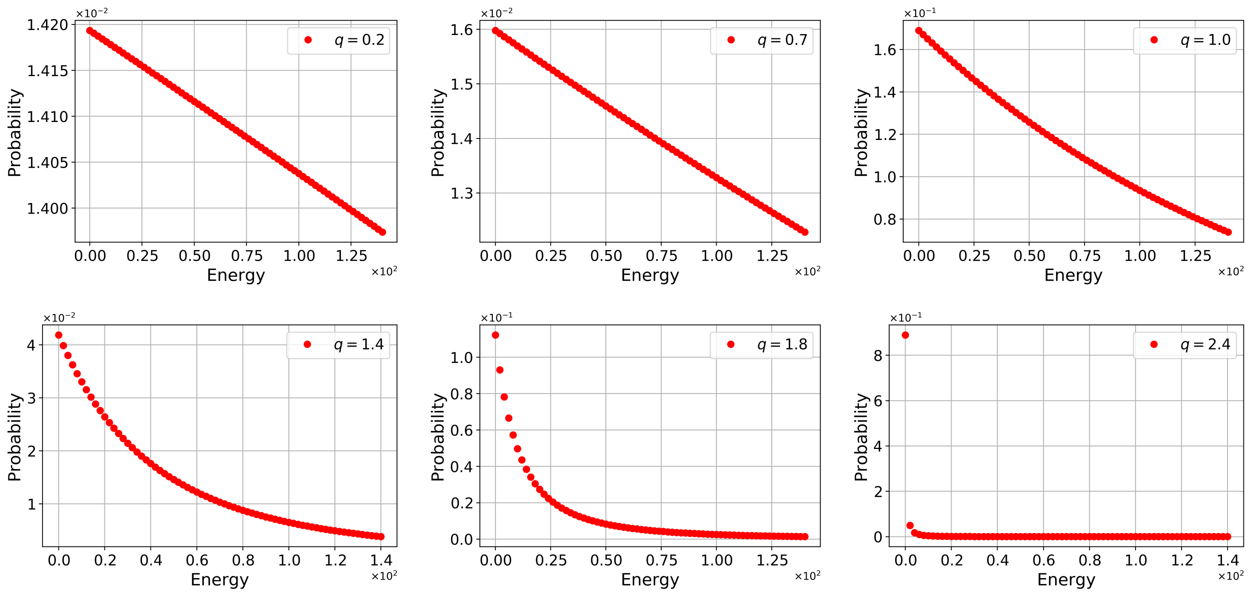

Figure 5. q-parametric energy distributions for the Hamiltonian of the form $H(\rho) \sim \kappa_1 \rho$

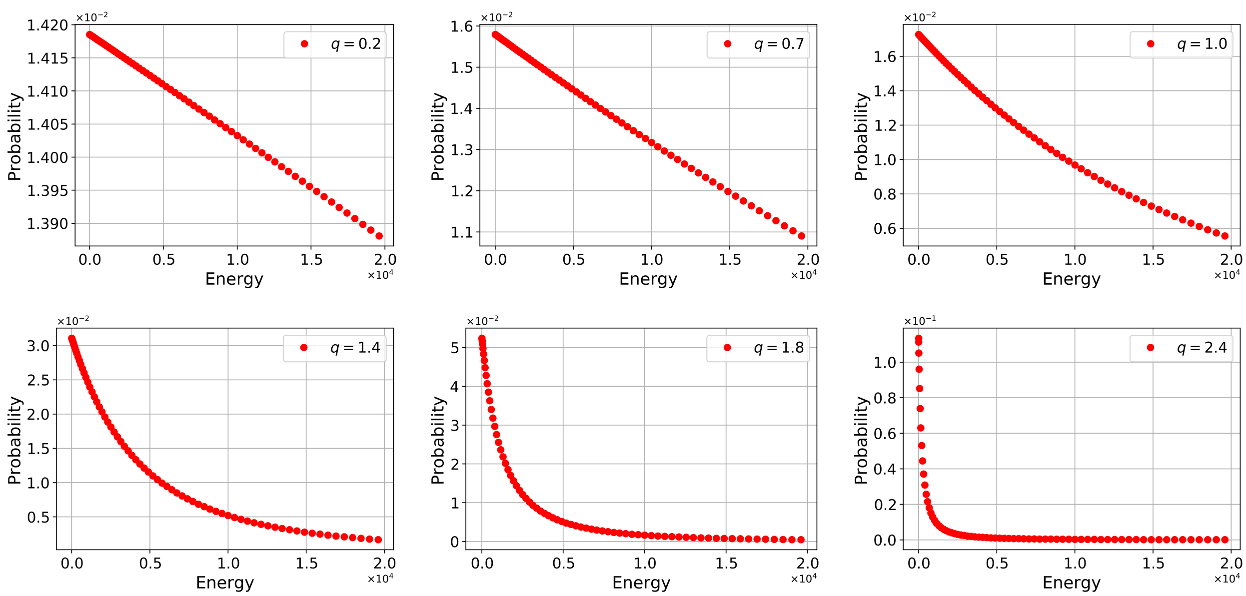

Figure 6. q-parametric energy distributions for the Hamiltonian of the form $H(\rho) \sim \kappa_2 \rho^2$

Regardless of the Hamiltonian type, the q-parametric family of energy characteristics has a number of common properties:

- in the range of $q \in [0, 0.8)$ the dependence of the population decreases linearly with increasing level energy, which is consistent with the spectra of the observed fluctuation processes and is typical for fractal and multifractal systems,
- in the values range of $q \in [2, 2.7)$ the dependence takes the hyperbola form
- in the values range of $q \in [0.9, 1.4)$ the dependence can be approximated by the Boltzmann exponent.

In fact, by the energy distribution shape, it is possible to determine the q-strain value and determine the degree of thermal nonequilibrium in the system by the relative dispersion of the temperature distribution function.

6. Q-PARAMETRIC EQUATIONS IN THE GASDYNAMIC APPROXIMATION

Let's consider the atmospheric path as a dynamic non-extensive system in which an unsteady distribution of particles in phase space is realized $f(\vec{r}, \vec{v}; t)$. The probability distribution function is normalized, the element of the phase space volume $\vec{z} = (\vec{r}, \vec{v})$. Let's introduce the entropy functional determined by the distribution function $f(\vec{z}; t)$:[15]

$$S_q\left[f\right] = -\frac{k_B}{1-q}\int (f(z) - (f(z)^q)dz \tag{16}$$

Let it be necessary to experimentally determine the macroscopic value of the q-system – $\langle \Theta_q \rangle$. Perform averaging of the corresponding microscopic value over the q-deformed distribution.

$$\langle \Theta_q \rangle \equiv \int \Theta(\vec{r}; t) f(z)^q dz \tag{17}$$

Note that in this case, the renormalization of the obtained value is not performed. This approach is typical for Curado Tsallis statistics.[8]

Let's define a number of q-parameters that determine the movement of gas flows:

– q - the number density of particles,

$$n_q(\vec{r}; t) \equiv \int f(z)^q d\vec{v}; \tag{18}$$

– q - the mass density

$$\rho_q(r; t) \equiv m n_q(\vec{r}; t), \tag{19}$$

where m is the particle mass;

q is the hydrodynamic velocity of the volume element,

$$\vec{u}_q(r; t) = \frac{1}{\rho_q(r; t)} \int m\vec{v} f(z)^q d\vec{v}; \tag{20}$$

specific internal q - energy,

$$\vec{\varepsilon}_q(r; t) = \frac{1}{\rho_q(r; t)} \int \frac{m}{2} |\vec{v} - \vec{u}_q|^2 f(z)^q d\vec{v}. \tag{21}$$

Using q-deformed variables, can obtain a system of q-hydrodynamic equations:

$$\frac{d\rho_q}{dt} + div(\rho_q \vec{u}_q) = 0, \tag{22}$$

$$\frac{d(\rho_q \vec{u}_q)}{dt} + Div(\vec{P}_q + \rho_q \vec{u}_q \vec{u}_q) = 0, \tag{23}$$

$$\frac{d(\rho_q \varepsilon_q)}{dt} + div(\vec{J}_q + \rho_q \varepsilon_q \vec{u}_q) + \vec{P}_q : Grad(u_q) = 0, \tag{24}$$

here $\vec{P}_q$ – stress tensor, $\vec{J}_q$ – heat flow. More details about the properties of the solutions of the written system of equations can be found in.[15]

7. LYAPUNOV EXPONENTS FOR TIME SERIES OF POSITIONAL CHARACTERISTICS

The determination of the chaotic process class is possible based on the Lyapunov exponents spectrum of equidistant time series of positional characteristics. To determine the dimensionality of the phase space, we use the nearest neighbors algorithm (NN)[17] in combination with the verification of surrogate data. To determine the maximum Lyapunov exponent, the Kantz algorithm is used.[18] In Fig.7 and Fig.8 presents three-second sweeps for the maximum Lyapunov exponent obtained by the sliding window method for a separate video sample.[19]

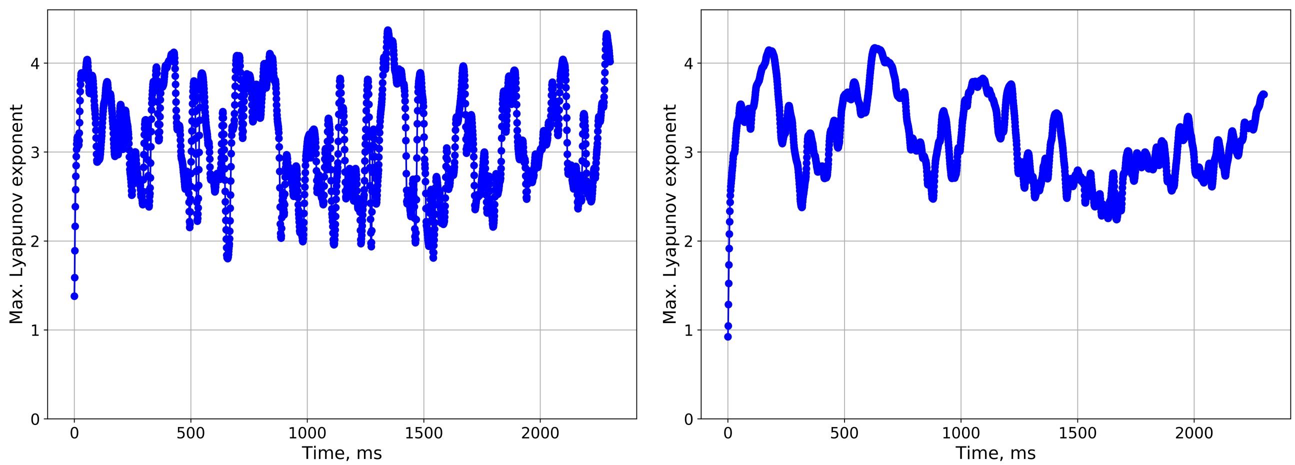

Figure 7. Sweeps of Lyapunov exponents for xC, yC offsets within the same video series

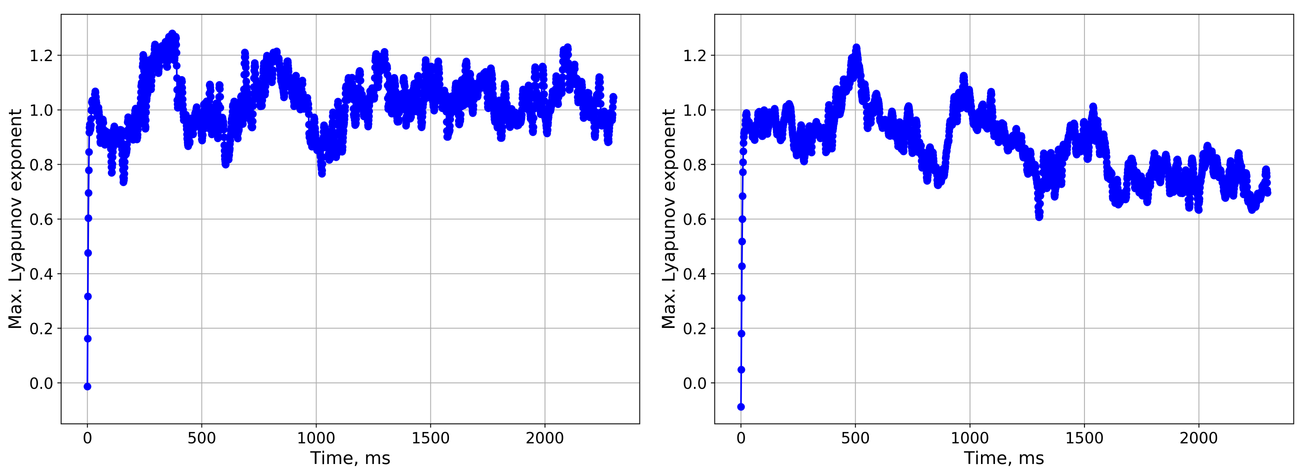

Figure 8. Sweeps of Lyapunov exponents for drift velocities vxC, vyC within the one video series

Significant non-stationarity of the observed values of the maximum Lyapunov exponent indicates a hyperchaotic mode of the system motion in phase space. To more accurately limit the class of available modes, let's consider the full range of Lyapunov exponents of the system under study in the scale of one video sample duration.The number of Lyapunov exponents coincides with the number of freedom degrees in the phase space. This number can change in different parts of the phase trajectory. In Fig.9 values of phase space dimensions for the analyzed parameters are presented. In Fig. 10 semidiurnal sweeps of the spectrum components of Lyapunov exponents are presented.

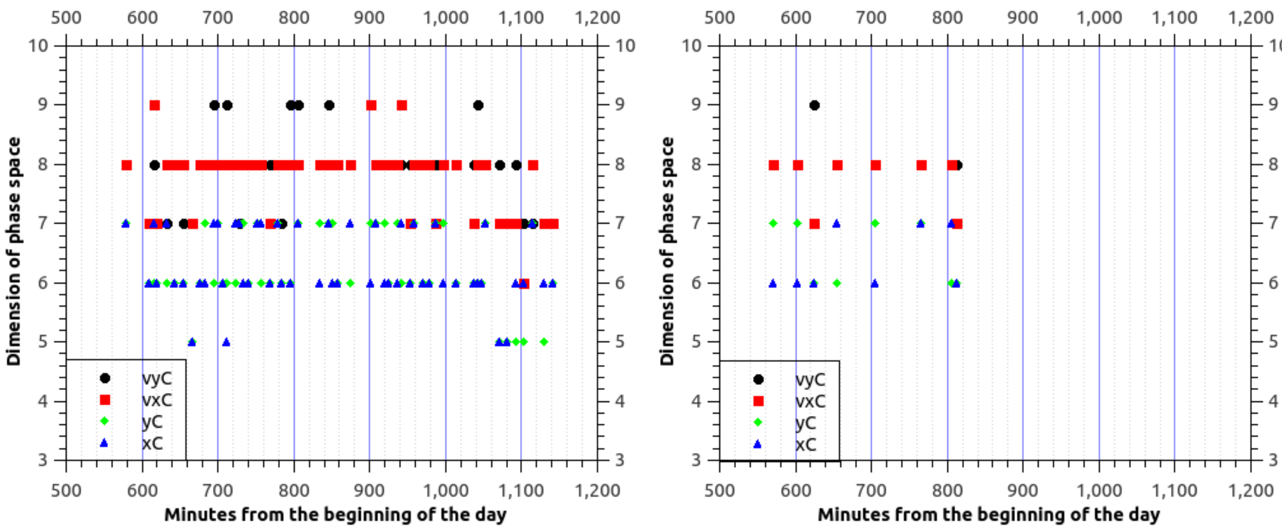

Figure 9. Sweep of phase space dimension values for various positional parameters of the wave beam center energy

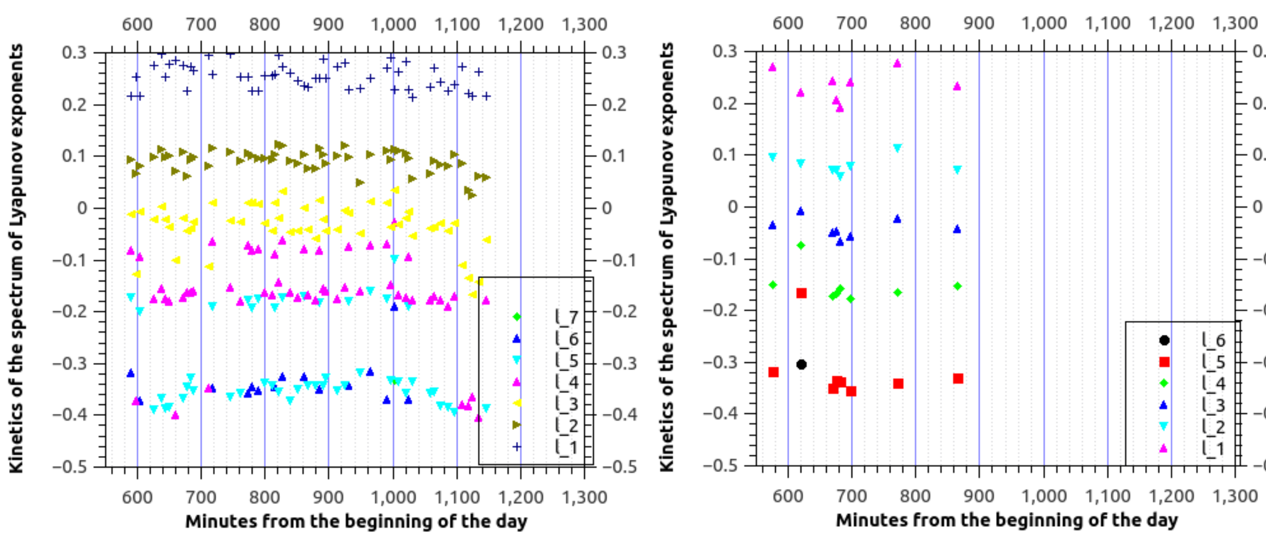

Figure 10. Sweep of the Lyapunov exponents for the horizontal displacement of the wave beam center energy

In almost all video series, the spectrum of Lyapunov exponents contains at least two positive definite components. The detected relatively weak component variation requires additional experimental analysis in the observation time interval. In a first approximation, the observed spectrum can be considered quasistationary and reflecting properties of convective flows in the selected time interval.

Conclusion

Let's formulate the main results of the experimental study:

- The multimodal distribution function for the recorded realizations of the displacement vector components and the drift vector of the energy-bearing center collimated wave beam can justify the use of Tsallis non-extensive thermodynamics, which allows us to control the fraction of states with low and high probability.

The thermodynamics and kinetics of complex systems based on the q-deformed Tsallis entropy, where q is the measure of non-additivity, predicts asymptotically power-law statistical distributions that go over into the exponential distribution in the limit $q \to 1$. It is these characteristics that are observed in the experimental series.

- The q-entropy of the positional parameters' statistical ensemble is informative in assessing of thermal nonequilibrium degree of a multicomponent system and can be used as a measure of the non-stationarity, spatial inhomogeneity, and nonequilibrium of the optical path. For $q \to 0$, the Tsallis entropy value coincides with the number of available states of the ensemble under study, determined by the spatial discretization conditions of the registration system. Such characteristic can be used for calibrating digital recorders.

- The considered method for the analysis of q-deformed characteristics includes an analysis of escort distributions, variation kinetics of the q-entropies set and energy distributions. Based on escort distributions, the experimentally observed ensemble-average parameters included in the state equations and the process equation can be calculated – the average q-density of gas particles, q-velocity of gas drift in the current tube, q-density of internal energy.

- On the microscale of time in hundreds of milliseconds, the maximum Lyapunov exponent varies greatly. However, with the change of timescale to more than 1 second, the variations decay and relatively weakly change in time during daylight hours. The observed positive values of the Lyapunov exponent make it possible to attribute the phase trajectories of positional characteristics to a specific type of chaotic regime – hyperhaos.

ACKNOWLEDGMENTS

The work was supported by State Theme "Wave Beams and Pulses in the Nonuniform and Stratified Media" AAAA-A17-117121890022-8.

REFERENCES

[1] Kolesnichenko, A. V. and Chetverushkin, B. N., "Derivation of hydrodynamic and quasi-hydrodynamic equations for transport systems based on statistics of tsallis," *Preprints of the Keldysh Institute of Applied Mathematics* , 8–32 (2014).

[2] Kolesnichenko, A. V., "To the construction of the thermodynamics of quantum nonextensive systems in the framework of the statistics of tsallis," *Preprints of the Keldysh Institute of Applied Mathematics* , 16–44 (2019).

[3] Tsallis, C., [*Introduction to nonextensive statistical mechanics: approaching a complex world*], Springer Science & Business Media (2009).

[4] Abe, S., "Stability of tsallis entropy and instabilities of rényi and normalized tsallis entropies: A basis for q-exponential distributions," *Physical Review E* **66**(4), 046134 (2002).

[5] Bashkirov, A. and Vityazev, A., "Information entropy and power-law distributions for chaotic systems," *Physica A: Statistical Mechanics and its Applications* **277**(1-2), 136–145 (2000).

[6] Bashkirov, A. G., "Renyi entropy as a statistical entropy for complex systems," *Theoretical and Mathematical Physics* **149**(2), 1559–1573 (2006).

[7] Tsallis, C., "Possible generalization of boltzmann-gibbs statistics," *Journal of statistical physics* **52**(1-2), 479–487 (1988).

[8] Curado, E. M. and Tsallis, C., "Generalized statistical mechanics: connection with thermodynamics," *Journal of Physics a: mathematical and general* **24**(2), L69 (1991).

[9] Mariz, A. M., "On the irreversible nature of the tsallis and renyi entropies," *Physics Letters A* **165**(5-6), 409–411 (1992).

[10] Matsak, I., Kapranov, V., Tugaenko, V. Y., Sergeev, E., Babanin, E., and Suhareva, N., "Super narrow beam shaping system for remote power supply at long atmospheric paths," in [*Laser Resonators, Microresonators, and Beam Control XIX*], **10090**, 100900U, International Society for Optics and Photonics (2017).

[11] Babanin, E., Suhareva, N., Vokhnik, O., Kapranov, V., Matsak, I., and Tugaenko, V., "Positional characteristics of generalized decentered elliptical gaussian beams propagating through extended atmospheric paths," in [*2017 Days on Diffraction (DD)*], 24–30, IEEE (2017).

[12] Umarov, S., Tsallis, C., and Steinberg, S., "On a q-central limit theorem consistent with nonextensive statistical mechanics," *Milan journal of mathematics* **76**(1), 307–328 (2008).

[13] Zaripov, R., "Changes in the entropy and the tsallis difference information during spontaneous decay and self-organization of nonextensive systems," *Russian physics journal* **44**(11), 1159–1165 (2001).

[14] Zaripov, R., "On thermodynamic equilibrium of nonextensive systems," *Technical physics* **51**(11), 1393–1397 (2006).

[15] Kolesnichenko, A. V., "To the construction of the thermodynamics of non-additive media on the basis of the statistics of tsallis–mendes–plastino," *Preprints of the Keldysh Institute of Applied Mathematics* , 23–28 (2018).

[16] Kolesnichenko, A. V., "Modification in the framework of nonadditive tsallis statistics of the gravitational instability criterions of astrophysical disks," *Matematicheskoe modelirovanie* **28**(3), 96–118 (2016).

[17] Cao, L., "Practical method for determining the minimum embedding dimension of a scalar time series," *Physica D: Nonlinear Phenomena* **110**(1-2), 43–50 (1997).

[18] Hegger, R., Kantz, H., and Schreiber, T., "Practical implementation of nonlinear time series methods: The tisean package," *Chaos: An Interdisciplinary Journal of Nonlinear Science* **9**(2), 413–435 (1999).

[19] Rosenstein, M. T., Collins, J. J., and De Luca, C. J., "A practical method for calculating largest lyapunov exponents from small data sets," *Physica D: Nonlinear Phenomena* **65**(1-2), 117–134 (1993).